

Resonant Inelastic X-Ray Scattering from Valence Excitations in Insulating Copper Oxides

P. Abbamonte,^{1,2,*} C. A. Burns,³ E. D. Isaacs,² P. M. Platzman,² L. L. Miller,⁴ S. W. Cheong,² and M. V. Klein¹

¹*Department of Physics, University of Illinois, 1110 W. Green Street, Urbana, Illinois 61801*

²*Bell Laboratories, Lucent Technologies, 600 Mountain Avenue, Murray Hill, New Jersey 07974*

³*Department of Physics, Western Michigan University, Kalamazoo, Michigan 49008*

⁴*Ames Laboratory, Ames, Iowa 50011*

(Received 7 October 1998)

We report resonant inelastic x-ray measurements of insulating La_2CuO_4 and $\text{Sr}_2\text{CuO}_2\text{Cl}_2$ taken with the incident energy tuned near the Cu K absorption edge. We show that the spectra are well described in a shakeup picture in third-order perturbation theory which exhibits both incoming and outgoing resonances and demonstrate how to extract a spectral function from the raw data. We conclude by showing \mathbf{q} -dependent measurements of the charge transfer gap.

PACS numbers: 78.70.Ck, 71.20.-b, 74.25.Jb

Inelastic x-ray scattering has shown promise as a practical probe of electronic excitations in condensed matter because of its broad kinematic range and direct coupling to the electron charge. However, since x rays are strongly absorbed in high density materials, successful applications of the technique have been limited to low- Z systems [1–5].

Several recent studies [6–9] have shown that by tuning the incident energy near an x-ray absorption edge a Raman effect could be measured, despite the high absorption, because of the resonant enhancement. These studies have emphasized the role of Coulomb interactions in the scattering process. Since it involves coupling between highly excited virtual states and strongly correlated valence states, it is important to characterize the resonance process well for the technique to be useful.

With emphasis on systematics, we have measured resonant inelastic x-ray scattering at moderate resolution ($\Delta E = 0.9$ eV) near the Cu K absorption edge in the high- T_c parent insulator La_2CuO_4 (LCO) as a function of incident photon energy. Based on the changes of inelastic intensity and peak position with incident energy we show that the scattering is well described in a “shakeup” picture in third-order perturbation theory [10]. We also present higher resolution measurements ($\Delta E = 0.45$ eV) on another insulator, $\text{Sr}_2\text{CuO}_2\text{Cl}_2$ (SCOC), as a function of momentum transfer, \mathbf{q} , which show some new features, such as the 2 eV optical charge transfer gap.

Experiments were carried out at the X21 wiggler line at the National Synchrotron Light Source and the 3ID (SRI-CAT) undulator line at the Advanced Photon Source. At X21 the energy resolution was 0.45 eV and typical count rates were 0.4 Hz. At 3ID with 0.9 eV resolution 9 Hz was typical. The scattered light was collected with a spherical, diced, Ge(733) analyzer and imaged onto a detector. Energy analysis was done by rotating the analyzer and translating the detector in coincidence. The momentum transfer was varied by rotating the entire apparatus around the scattering center (exact experimental geometries are indicated in the figure captions).

The LCO and SCOC crystals were grown by techniques described previously [11,12]. They were characterized with a spectroscopic ellipsometer to assure surface quality.

In the upper panel of Fig. 1 we show inelastic x-ray spectra from La_2CuO_4 at fixed \mathbf{q} for 16 different incident x-ray energies across the Cu K absorption edge. Since the overall absorption change across the edge is only 14% (x-ray absorption being dominated by the La atoms) corrections for sample self-absorption did not significantly alter the line shapes. So shown here are the raw spectra. The strong peak at zero energy loss is elastic scattering. The energy gain side (negative energy loss) shows a background of 12 counts per minute. The principal feature of each curve is a single peak, seen previously in Nd_2CuO_4 [8], whose position, intensity, and line shape vary greatly as a function of incident energy.

We summarize the resonant behavior in the lower frame of Fig. 1 where the inelastic peak height (open circles) and position (filled circles) are plotted against *incident* energy. The thick line is the Cu K fluorescence yield which shows the location of the edge (a localized $\text{Cu } 1s \rightarrow 4p$ transition). The peak height shows two maxima, the stronger of which correlates with the peak of the edge and the weaker with the pre-edge shoulder. In both cases the maximum is offset from the absorption peak by about 2.5 eV.

The peak *position* shifts nonlinearly with incident energy; below and above a resonance it is roughly linear while near a resonance it plateaus. This behavior differs fundamentally from a classic Raman effect, in which one expects a linear peak shift with unit slope with a gradual rise in intensity below a resonance and saturation above [13].

Independent of any model, this type of low energy loss scattering leads to excited states of the valence electron system in the absence of core excitations. However, because one is near the $1s$ absorption threshold of Cu the scattering proceeds through a set of almost real, highly excited (9 keV) intermediate states, which have a $1s$ core hole and an extra electron excited in a

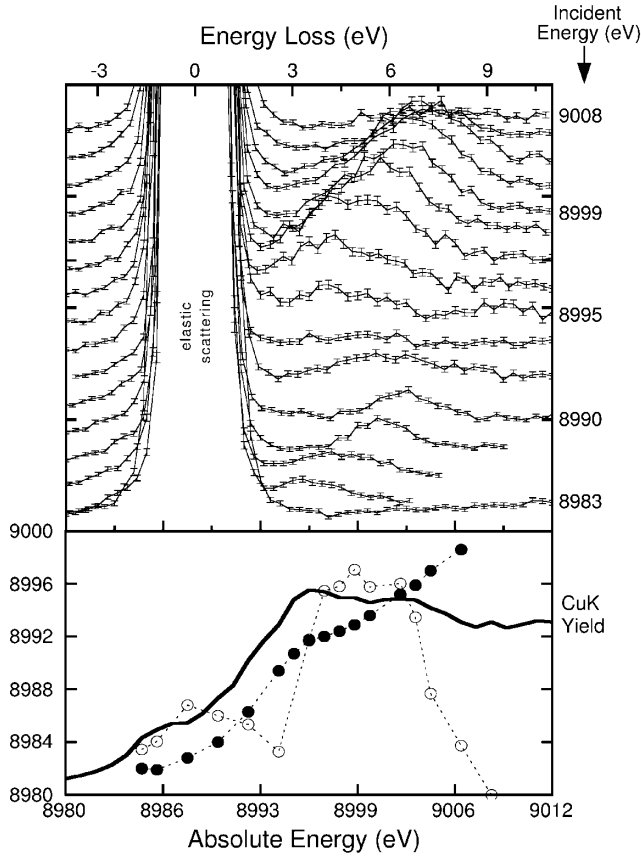


FIG. 1. Resonance profile for La_2CuO_4 taken at 3ID with $\hat{\epsilon}_i \parallel \hat{a}$ and $\mathbf{q} = 1.27 \text{ \AA}^{-1}$ parallel to \hat{c} . The upper frame shows the raw spectra plotted against *transferred* energy (curves are offset for clarity). In the lower frame the open and filled circles are the inelastic peak height and position, respectively, plotted against *incident* energy. The black line is the fluorescence yield which peaks at the $\text{Cu } 1s \rightarrow 4p$ energy.

localized $4p$ state ($\bar{1}s4p$). When the highly excited intermediate state disappears, it leaves behind low-lying valence excited states—in principle, conserving energy and crystal momentum.

One must describe these many-body intermediate states, i.e., their matrix elements as well as their off-shell weight, in order to characterize the coherent, second-order process. Different groups have resorted to different approximation schemes. Starting with N valence electrons in a small cluster, Tanaka, Kayanuma, and Kotani [14] describe the intermediate states as a set of $N + 1$ interacting electrons in the presence of a rigid impurity—the Anderson impurity model. This treatment assumes that the core state is suddenly created, and that it can be treated as a fixed, external potential. It emphasizes the multiplet coupling among the $N + 1$ electrons and is done numerically in exact diagonalization with a large number of basis functions.

Taking a more analytic approach, Platzman and Isaacs [10] treat the many-body problem by describing Coulomb interactions among electrons in a series of perturbation diagrams [15]. This approach assumes that interactions

can be taken to be weak for a suitable choice of basis functions *or* that one can sum enough terms in perturbation theory to include the important physics. They argue that near a sharp, dipole-allowed transition the dominant term occurs in third order. Writing it out explicitly one arrives at

$$M = \sum_{\bar{1}s,4p} \frac{M_{\text{em}} M_{\text{Coul}} M_{\text{abs}}}{(\omega_s - E_{\bar{1}s,4p} + i\gamma_K)(\omega_i - E_{\bar{1}s,4p} + i\gamma_K)}. \quad (1)$$

In this expression the sum is on all possible states of the $1s$ hole and $4p$ electron, $E_{\bar{1}s,4p}$ is their energy, and γ_K is their inverse lifetime. The numerator contains matrix elements for absorption, $M_{\text{abs}} = (e/mc) \langle \bar{1}s4p | \mathbf{p} \cdot \hat{\mathbf{A}} | \mathbf{k}_i \rangle$, emission, $M_{\text{em}} = (e/mc) \langle \mathbf{k}_s | \mathbf{p} \cdot \hat{\mathbf{A}} | \bar{1}s4p' \rangle$, and Coulomb interaction between the core and valence states, $M_{\text{Coul}} = \int d\mathbf{x} d\mathbf{x}' \langle \bar{1}s'4p' | f | \hat{\rho}(\mathbf{x}) \hat{\rho}(\mathbf{x}') | \mathbf{x} - \mathbf{x}' | | \bar{1}s4p; i \rangle$. \mathbf{k}_i and \mathbf{k}_s are the incident and scattered photon momenta (i.e., $\mathbf{q} = \mathbf{k}_i - \mathbf{k}_s$) and $\omega = \omega_i - \omega_s$ is the energy loss.

Physically this expression represents the following. The incident photon, with energy tuned to the Cu K absorption edge, creates a virtual $\bar{1}s4p$ pair on a Cu site. This pair is bound as an exciton by the Coulomb interaction [not included in Eq. (1)] and so is nondispersive. It takes up the momentum of the incident photon, 4.55 \AA^{-1} , and scatters off the valence electron system. When the exciton recombines, the emitted photon reflects the energy and momentum imparted to the system. This is commonly called a shakeup process, which to first order in the Coulomb interaction is given by Eq. (1).

To get a transition rate we square the quantity (1) and perform an incoherent sum on final states. We postulate that the intermediate states are approximately degenerate with energy $E_{\bar{1}s,4p} = E_K$ (since they are spatially localized), which allows factoring of the energy denominators from the sum. We arrive at

$$w = \frac{S_K(\mathbf{q}, \omega; \hat{\epsilon}_i, \hat{\epsilon}_s)}{[(\omega_i - E_K)^2 + \gamma_K^2][(\omega_s - E_K)^2 + \gamma_K^2]}, \quad (2)$$

where

$$S_K = \frac{2\pi}{\hbar} \sum_f \left| \sum_{\bar{1}s,4p} M_{\text{em}} M_{\text{abs}} M_{\text{Coul}} \right|^2 \delta(\omega - E_f + E_i), \quad (3)$$

and $\hat{\epsilon}_i$ and $\hat{\epsilon}_s$ are the polarizations of the incident and scattered photons. The two Lorentzians in (2) are incoming and outgoing resonances in the photon frequency, so we see that this treatment is completely analogous to third-order optical Raman scattering from phonons in semiconductors, in which the scattering is described by a single operation of the *electron-phonon* interaction on a virtual *valence* electron-hole pair [16]. The two resonances formally come about the same way.

The central result of this paper is Eq. (2). It says that, within our approximation, all the very different spectra

in Fig. 1 derive from the same fundamental quantity, S_K , which depends on the *difference* $\omega = \omega_i - \omega_s$ rather than on ω_i and ω_s independently. A way to test this result would be to take the curves from Fig. 1, divide each by its respective denominator from Eq. (2), and see if they all collapse to the same function.

In Eq. (2) we assumed that we are near a single resonance, so we take the nine highest curves from Fig. 1 (around the second peak in the resonance profile) and subtract their background and elastic scattering. We use E_K and γ_K as flexible parameters and divide each spectrum by its respective denominator. Using a nonlinear fitting algorithm, we adjust the values of E_K and γ_K to minimize the total variation (the χ^2 summed over all points and all spectra) among the curves, irrespective of the resulting shape. For the values $E_K = (8995.14 \pm 1.61)$ eV and $\gamma_K = (2.38 \pm 0.542)$ eV we find that the spectra collapse onto a single curve, shown in Fig. 2.

The result for $S_K(\mathbf{q}, \omega; \hat{\epsilon}_i, \hat{\epsilon}_s)$ is a single peak at 6.1 eV energy loss and width of 3.9 eV. Referring to the cluster calculations of S  mon [17] we suggest that this feature is a transition from the b_{1g} ground state to an a_{1g} excitonic excited state composed of symmetric combinations of a central $\text{Cu}3d_{x^2-y^2}$ orbital and the surrounding $\text{O}2p_\sigma$ orbitals.

To illustrate what *qualitative* aspects of the data are captured by our fit, i.e., by the resonant denominators in (2), we take a single function for S_K , i.e., a fit to the collapsed data in Fig. 2 (thick line), combine it with the denominators in Eq. (2), and produce the model resonance profile shown in Fig. 3 (identical formatting to Fig. 1). The salient features are reproduced, including the peak shift with incident energy and the 2.5 eV offset. All this behavior comes from the energy denominators in (2) and is independent of the nature of the core state or the particular valence excitation.

In this simple shakeup description $S_K(\mathbf{q}, \omega; \hat{\epsilon}_i, \hat{\epsilon}_s)$ has an explicit relationship with $S(\mathbf{q}, \omega)$, the dynamical struc-

ture factor measured in nonresonant inelastic x-ray scattering [18]. This can be seen by writing out the matrix element M_{Coul} in momentum space, which (neglecting exchange between core and valence states) has the form

$$M_{\text{Coul}} = \sum_{\mathbf{G}} \frac{4\pi e^2}{|\mathbf{q} + \mathbf{G}|^2} F_{\bar{1}s4p}(\mathbf{q} + \mathbf{G}; \hat{\epsilon}_i) \langle f | \hat{\rho}_{v, \mathbf{q} + \mathbf{G}} | i \rangle. \quad (4)$$

Here $F_{\bar{1}s4p}(k)$ is the static x-ray form factor of the $\bar{1}s4p$ exciton. It is dependent implicitly on the incident polarization $\hat{\epsilon}_i$ since in the dipole approximation M_{abs} determines the spatial orientation of the $4p$. $\hat{\rho}_{v, \mathbf{q}}$ is the valence part of the many-body density operator $\hat{\rho}_{\mathbf{q}}$ and the sum in (4) is on all reciprocal lattice vectors, \mathbf{G} .

The quantity $\langle f | \hat{\rho}_{v, \mathbf{q}} | i \rangle$, when squared, multiplied by $\delta(\omega - E_f + E_i)$, and summed on final states, is identically the valence part of the dynamic structure factor $S(\mathbf{q}, \omega)$. Doing the sum on \mathbf{G} before squaring we find that $S_K(\mathbf{q}, \omega; \hat{\epsilon}_i, \hat{\epsilon}_s)$ is a superposition of many $S(\mathbf{q} + \mathbf{G}, \omega)$ functions, weighted by the form factor of the core states. Therefore, S_K can be thought of as a response function similar to S "projected" onto the form factor of the core state.

Finally we present some higher-resolution ($\Delta E = 0.45$ eV), \mathbf{q} -dependent spectra from the insulator $\text{Sr}_2\text{CuO}_2\text{Cl}_2$ (Fig. 4). The salient spectral features are three peaks: the same feature we saw in LCO (appearing

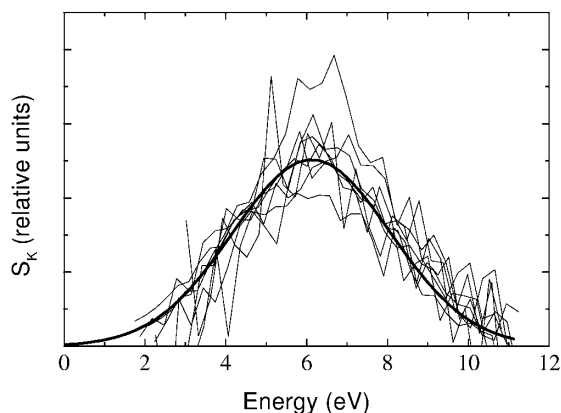


FIG. 2. The result of dividing energy denominators in (2) from the experimental spectra in Fig. 1. For $E_K = (8995.14 \pm 1.61)$ eV and $\gamma_K = (2.38 \pm 0.542)$ eV all spectra collapse onto a single curve. The thick line is a Gaussian fit.

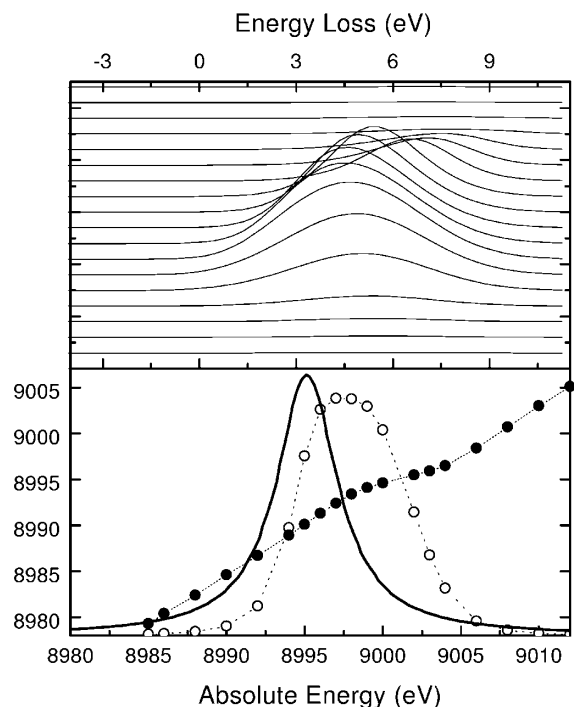


FIG. 3. A model resonance profile generated from the dark line in Fig. 2 and the two resonant denominators in Eq. (2). Formatting is identical to Fig. 1. The solid line is a simulated Cu K fluorescence yield showing the absorption peak. The continuum above the peak is omitted since it does not contribute to the resonance.

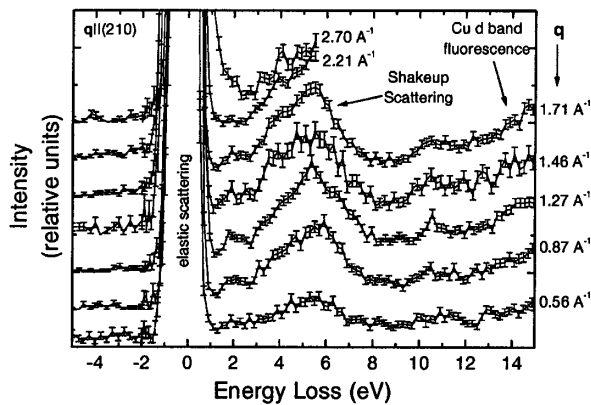


FIG. 4. Resonant spectra from $\text{Sr}_2\text{CuO}_2\text{Cl}_2$ as a function of \mathbf{q} , taken at X21 with both \mathbf{q} and $\hat{\epsilon}_i$ approximately parallel to the (210) crystallographic direction. The feature at 2 eV is the charge transfer gap, which changes shape and shifts with increasing \mathbf{q} .

here at about 5 eV), a feature at 2 eV which appears to shift and lose definition with \mathbf{q} , and a peak at 10.5 eV which is absent at low \mathbf{q} but which gains intensity as \mathbf{q} is increased. The 2 eV feature strongly resembles dipole-active charge transfer gap seen with optical reflectivity [19].

To summarize, we measured resonant inelastic x-ray scattering spectra at the Cu K edge in LCO and SCOC. From the resonance profile we deduce that the scattering can be described as a shakeup process in third order which, analogous to optical Raman scattering from phonons, exhibits incoming and outgoing resonances. The scattered intensity has the form of a doubly resonant form factor multiplied by a response function, $S_K(\mathbf{q}, \omega; \hat{\epsilon}_i, \hat{\epsilon}_s)$, which can be thought of as the dynamical structure factor projected onto the form factor of the intermediate core state.

The advantages of this shakeup description are (i) that it makes no assumption that the core state is rigid and so momentum conservation enters naturally and (ii) that it allows one, given certain knowledge of the intermediate state [i.e., $F_{\Gamma_{54p}}(\mathbf{k})$], to relate the scattering to a response function in terms of the valence electrons only. This description is useful when the core resonance is sharp and well isolated, and when one is mostly interested in the valence electron spectrum and is willing to sacrifice a detailed multiplet description of the core states.

We gratefully acknowledge E. E. Alp, Z. Hasan, C.-C. Kao, V. I. Kushnir, P. L. Lee, H. L. Liu, A. T. Macrander,

G. A. Sawatzky, M. Schwoerer-Böhning, M. E. Símón, S. K. Sinha, J. P. Sutter, T. Toellner, and C. Varma. This work was supported by the NSF under Grant No. DMR-9705131 and by the U.S. Department of Energy, Basic Energy Sciences, Office of Energy Research, under Contract No. W-31-109-ENG-38.

*Present address: Solid State Physics Lab, Nijenborgh 4, 9747AG Groningen, The Netherlands.

- [1] M. H. Krisch, F. Sette, C. Masciovecchio, and R. Verbeni, *Phys. Rev. Lett.* **78**, 2843 (1997).
- [2] J. P. Hill, C.-C. Kao, W. A. C. Caliebe, D. Gibbs, and J. B. Hastings, *Phys. Rev. Lett.* **77**, 3665 (1996).
- [3] H. Nagasawa, S. Mourikis, and W. Schülke, *J. Phys. Soc. Jpn.* **66**, 3139 (1997).
- [4] B. C. Larson, J. Z. Tischler, E. D. Isaacs, P. Zschack, A. Fleszar, and A. G. Eguiluz, *Phys. Rev. Lett.* **77**, 1346 (1996).
- [5] E. D. Isaacs, P. M. Platzman, P. Metcalf, and J. M. Honig, *Phys. Rev. Lett.* **76**, 4211 (1996).
- [6] E. D. Isaacs, *Ferroelectrics* **176**, 249 (1996).
- [7] C. C. Kao, W. A. L. Caliebe, J. B. Hastings, and J.-M. Gillet, *Phys. Rev. B* **54**, 16361 (1996).
- [8] J. P. Hill, C.-C. Kao, W. A. L. Caliebe, M. Matsubara, A. Kotani, J. L. Peng, and R. L. Greene, *Phys. Rev. Lett.* **80**, 4967 (1998).
- [9] S. M. Buterin *et al.*, *Phys. Rev. Lett.* **77**, 574 (1996).
- [10] P. M. Platzman and E. D. Isaacs, *Phys. Rev. B* **57**, 11107 (1998).
- [11] L. L. Miller, X. L. Wang, S. X. Wang, C. Stassis, D. C. Johnston, J. Faber, Jr., and C.-K. Loong, *Phys. Rev. B* **41**, 1921 (1990).
- [12] S.-W. Cheong *et al.*, *Solid State Commun.* **65**, 111 (1988).
- [13] P. Eisenberger, P. M. Platzman, and H. Winick, *Phys. Rev. B* **13**, 2377 (1976).
- [14] S. Tanaka, Y. Kayanuma, and A. Kotani, *J. Phys. Soc. Jpn.* **59**, 1488 (1990).
- [15] For yet another treatment, see Faris Gel'mukhanov and Hans Ågren, *Phys. Rev. B* **57**, 2780 (1998), Sec. IV-B.
- [16] P. Y. Yu and M. Cardona, *Fundamentals of Semiconductors* (Springer-Verlag, Berlin, Heidelberg, New York, 1996), Sec. 7.2.8.
- [17] M. E. Símón, A. A. Aligia, C. D. Batista, E. R. Gagliano, and F. Lema, *Phys. Rev. B* **54**, R3780 (1996).
- [18] W. Schülke, in *Handbook on Synchrotron Radiation*, edited by G. Brown and D. E. Moncton (Elsevier, Amsterdam, 1991), Vol. 3.
- [19] A. Zibold, H. L. Liu, S. W. Moore, J. M. Graybeal, and D. B. Tanner, *Phys. Rev. B* **53**, 11734 (1996).